Modeling Superconducting Components of the Electric Aircraft

Ali Khonya, Mathias Noe, Wescley T. B. de Sousa, Frederick Berg, and Michael Cooper

***Abstract*—Electrification of the mobility sector is at the center of attention to reduce CO_2 emissions and mitigate man-made climate change. At present, commercial air travel is responsible for around 2.4% of the annual global carbon emissions. This is a motivation behind developing fully-electric, zero-emission aircraft. The advantages of superconductivity, including compactness, low weight, and high efficiency, make this technology a promising choice to accelerate the transition to electric aircraft. An electric aircraft's powertrain might include motors, converters, DC and AC cables, batteries, fuel cells, fault current limiters, power generators, and fuel storage. The higher the total power of the electric aircraft, the more interesting it is to use superconducting devices. This work models the overall electric powertrain with MATLAB/SIMULINK. One component is a resistive superconducting fault current limiter which is modeled via an electrical-thermal lumped-parameter method in MATLAB. Moreover, the electrical-thermal lumped-parameter, one-dimensional, and two-dimensional modeling of superconducting DC cables is developed using MATLAB programming and compared. In addition, the configurable MATLAB SIMULINK models of these components can be integrated in other electric systems.**

***Index Terms*—Electric aircraft, superconducting DC cable, superconducting fault current limiter.**

I. Introduction

THE growing emphasis on addressing climate change and reducing CO_2 emissions has brought considerable focus to the electrification of transportation. In 2021, commercial aviation was responsible for approximately 2.4% of the world's carbon emissions [1]. Considering the projected substantial increase in aircraft production [2], this contribution is expected to grow significantly. The aerospace industry has set ambitious goals, including the EU Flightpath 2050 plan, which aims to achieve a 75% reduction in carbon emissions [3]. One potential solution that has emerged is the concept of full electric aircraft (FEA), which could offer a viable means to achieve this objective [4].

Superconductors provide benefits in power systems compared to conventional alternatives in terms of their compactness, lightweight nature, and higher efficiency [5], [6]. At present, various electrical components, including fault current limiters (FCLs), cables, machines, and transformers have already reached a high technical maturity level. As a result, implementing a superconducting powertrain in electric aircraft seems viable and enables the aviation industry to build the first demonstrators [4], [5], [6].

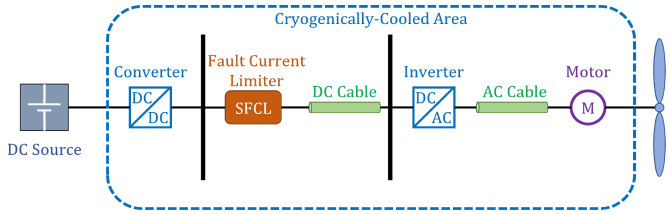

Fig. 1. Schematic of the electric aircraft superconducting powertrain [8].

The possible powertrain design consists of multiple components, starting with the DC source and extending to the propeller's motor [7], [8]. Situated between these components are converters for voltage amplitude variation and conversion and superconducting DC and AC cables to ensure efficient current transportation to the motor. Moreover, a resistive superconducting fault current limiter (RSFCL) is incorporated into the system to prevent sudden rises in current caused by potential short circuits. The schematic of the proposed powertrain is shown in Fig. 1. For this study, liquid nitrogen (LN_2) at a temperature of 77 K is the cooling medium for the system.

This work aims to develop a complete MATLAB and SIMULINK model of an electric aircraft powertrain. At first step, the paper focuses on modeling two key components in this powertrain and comparing the models for each one: the resistive superconducting fault current limiter (RSFCL) and the superconducting DC cable. The electrical-thermal behavior of both components is thoroughly analyzed, and the methodology for simulating their behavior is outlined. The simulation results, which provide insights into the performance and behavior of the RSFCL and superconducting DC cable, are then presented and discussed.

II. Study Case

The simplified study case network consists of a 300 V DC source, a bipolar transmission line, and a load, with a fault occurring at the load location. The schematic of this case is provided in Fig. 2. In nominal conditions, 1.5 kA current flows through the network, and the steady-state short circuit current due to the pole-to-pole fault at the load location is 15 kA. In the

Ali Khonya, Mathias Noe, and Wescley T. B. de Sousa are with the Institute for Technical Physics, Karlsruhe Institute of Technology, 76131 Karlsruhe, Germany (e-mail: Ali.khonya@kit.edu).

Frederick Berg and Michael Cooper are with Airbus X-Labs, 82024 Taufkirchen, Germany.

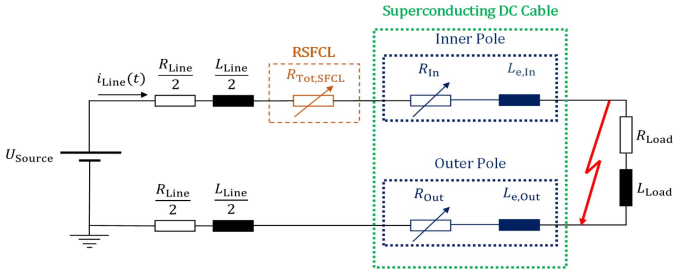

Fig. 2. Schematic of the study case network with both RSFCL and bipolar DC cable.

TABLE I
PROPERTIES OF THE CONSIDERED HTS TAPES FOR THE RSFCL AND DC CABLE.

Parameter	Specification		Unit
	RSFCL	Cable	
Tape Width	12	4	mm
Tape Length	8.5	50	m
Copper Thickness	-	40	μm
Silver Thickness	4	3	μm
REBCO Thickness	1	2	μm
Hastelloy Thickness	100	75	μm
Tape Total Thickness	105	120	μm
Tape Critical Temperature	92	92	K
Tape Critical Current	550	210	A

simulation of the bipolar DC cable, a stand-alone model without the existence of the RSFCL is analyzed, then the combination of both components is investigated as seen in Fig. 2.

III. RESISTIVE SUPERCONDUCTING FAULT CURRENT LIMITER

In this study, a resistive superconducting fault current limiter is considered. The RSFCL with a total resistance of $R_{\text{Tot,SFCL}}$ is placed in series with other network elements as shown in Fig. 2. This study considers a High Temperature Superconducting (HTS) REBCO tape comprising three layers: one for REBCO as superconductor, and the other two are silver (Ag) as a stabilizer and Hastelloy (Hy) as a substrate. The properties of this tape are described in Table I. Considering the 1.5 kA nominal current flowing through the SFCL, three HTS tapes need to be connected in parallel. To model the RSFCL, the lumped-parameter method considering its electrical and thermal characteristics is used [9].

Electrical Characteristic The equivalent electrical circuit of an RSFCL highlighting the resistance of each layer of the tapes is depicted in Fig. 3. The parallel resistance law is applied to calculate the resistance of a single tape R_{Tape} from resistances of tape sub-layers: resistance of the silver layer R_{Silver}, resistance of the REBCO superconductor layer R_{REBCO}, and resistance of the Hastelloy substrate layer $R_{\text{Hastelloy}}$. Furthermore, when multiple tapes are employed in an SFCL (N tapes), assuming they have identical properties, resistances, and temperatures, the total resistance of the SFCL, $R_{\text{Tot,SFCL}}$ is also calculated from the resistance of one tape based on the same law. These equations are shown in (1).

$$\frac{1}{N \cdot R_{\text{Tot,SFCL}}} = \frac{1}{R_{\text{Tape}}} = \frac{1}{R_{\text{Silver}}} + \frac{1}{R_{\text{REBCO}}} + \frac{1}{R_{\text{Hastelloy}}} \tag{1}$$

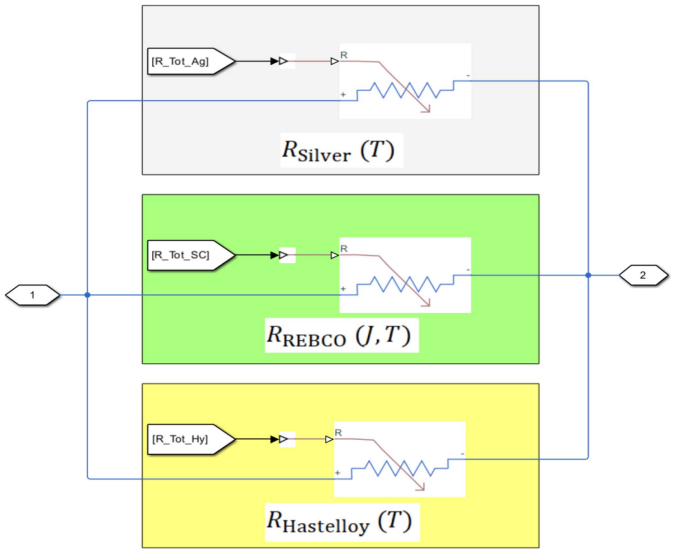

Fig. 3. Developed electrical schematic of the RSFCL in SIMULINK.

In contrary to the linear (with temperature T) behavior of the silver and Hastelloy layers with temperature [9], the resistance of the REBCO superconductor acts non-linearly and is calculated from its electric field E and current density J based on known E-J power law [9], [10].

Thermal Characteristic In this work, it is assumed that all tapes in the SFCL have the same temperature, and there is no temperature gradient within the tapes (T_{Silver}=T_{REBCO}=$T_{\text{Hastelloy}}$=T_{Tape}). Moreover, The coolant temperature remains constant at 77 K ($T_{\text{LN}_2} = 77$ K). The tape temperature T_{Tape} is then calculated with (2):

$$C_{\text{Tape}} \cdot \frac{\partial T_{\text{Tape}}}{\partial t} = P_{\text{Tape}} - P_{\text{c}} = R_{\text{Tape}} \cdot I_{\text{Tape}}^2 - P_{\text{c}} \tag{2}$$

with C_{Tape} as the tape heat capacity, P_{Tape} as the power loss in the tapes, and P_{c} as the cooling (convected) power by cooling fluid. The power loss in the tapes P_{Tape} can be calculated based on the tape current I_{Tape} and resistance R_{Tape} as shown in this equation. The cooling power P_{c} is dependent on the heat transfer conditions; The calculation of P_{c} in non-adiabatic condition is shown in (3):

$$P_{\text{c,Non-Adiabatic}} = 2h_{\text{c,LN}_2} \cdot w_{\text{Tape}} \cdot l_{\text{Tape}} \cdot \Delta T \tag{3}$$

with $h_{\text{c,LN}_2}$ as LN_2 convective heat transfer coefficient, w_{Tape} as tape width, l_{Tape} as tape length, and ΔT as the difference between T_{Tape} and T_{LN_2}. The convective heat transfer coefficient $h_{\text{c,LN}_2}$ is calculated with the following equation, where the values of α_{i} can be found in [9]:

$$h_{\text{c,LN}_2} = \begin{cases} 2170 & ;\Delta T \leq 3.2 \\ \frac{\sum_{i=0}^{5} \alpha_i \cdot \Delta T^i}{\Delta T} & ;3.2 < \Delta T \leq 28 \\ \frac{3970+\Delta T}{\Delta T} & ;\Delta T > 28 \end{cases} \tag{4}$$

Initially, the temperature of all tapes is 77 K, and the temperature increase in the tapes ΔT_{Tape} is calculated based on equation (2)

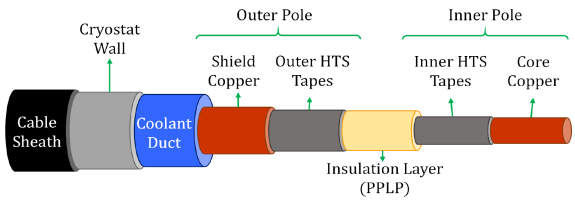

Fig. 4. Structure of the bipolar superconducting DC cable.

TABLE II
PHYSICAL GEOMETRY SPECIFICATIONS OF THE BIPOLAR SUPERCONDUCTING DC CABLE.

Parameter	Specification	Unit
Core Copper Diameter	10	mm
Outer Diameter of the Inner HTS Tapes	10	mm
PPLP Outer Diameter	15	mm
Outer Diameter of the Outer HTS Tapes	15	mm
Shield Copper Outer Diameter	18	mm
Coolant Duct Outer Diameter	28	mm
Cable Outer Diameter	30	mm
Cable Length	50	m

using the following equation, considering the time-step Δt:

$$\Delta T_{\text{Tape}} = \Delta t \cdot \left(\frac{R_{\text{Tape}} \cdot I_{\text{Tape}}^2 - P_{\text{c}}}{C_{\text{Tape}}} \right) \tag{5}$$

Assuming the same properties and resistance for all tapes, current is evenly distributed among the parallel tapes. An implicit numerical method is used to calculate the line current according to [9].

IV. SUPERCONDUCTING DC CABLE

In this work, a bipolar DC cable as depicted in Fig 4 is considered. The parameters R_{In} and R_{Out} represent the resistances of the inner and outer poles, and $L_{\text{e,In}}$ and $L_{\text{e,Out}}$ indicate their effective inductances. In [11], the formulas to calculate these inductances are given. The superconducting cable comprises several layers starting from the cable's center and extending towards the sheath including a core copper layer and a single layer of HTS tapes in the inner pole, and another layer of HTS tapes and shield copper in the outer pole. Furthermore, a Polypropylene Laminated Paper (PPLP) layer provides insulation between the poles. Finally, there is a coolant flowing duct within the cryostat. The detailed cable geometry is described in Table II. In this work, like RSFCL, LN_2 at 77 K is used to cool the superconductor. The HTS tape considered for this cable has a similar structure to the RSFCL tapes but with an additional copper sub-layer. The structure of this tape is depicted in Fig 3(b), and its properties are described in Table I. In this coaxial DC cable, 8 and 12 HTS tapes are considered for the inner and outer poles, leading to the inner and outer HTS tapes' critical currents being 1.68 kA and 2.52 kA.

The lumped-parameter (L-P) method can be used to simulate the superconducting cable in adiabatic condition, similar to the RSFCL. However, for modeling the cable in non-adiabatic conditions due to the heat conduction/convection between the layers, more advanced models like one-dimensional (1-D) or

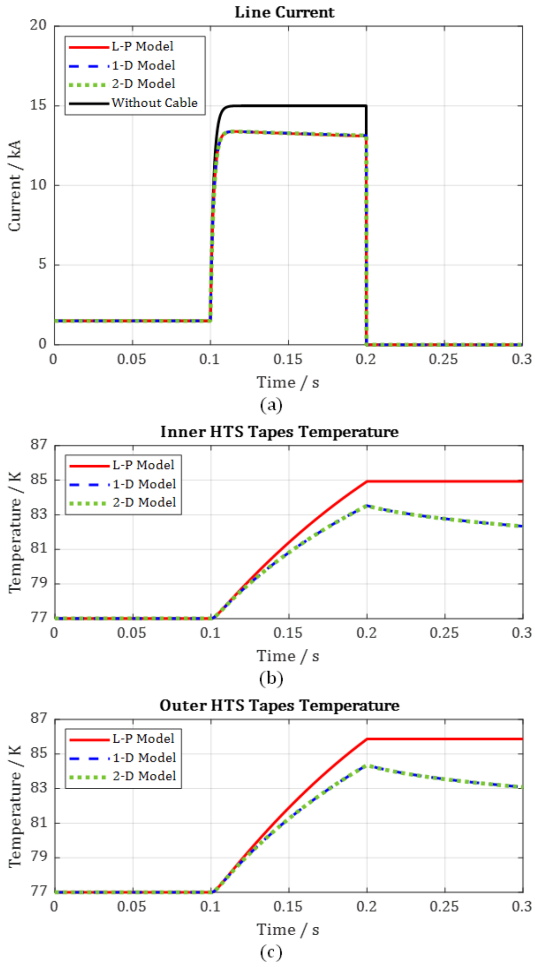

Fig. 5. Cable simulation results obtained from different models: (a) Line current. (b) Inner HTS tapes temperature. (c) Outer HTS tapes temperature.

two-dimensional (2-D) models are needed: the 1-D model indicates temperature calculation only along the cable radius, and in the 2-D model the temperature along both cable radius and length is calculated. A 2-D electrical-thermal model is developed using the finite difference method (FDM) according to [12] to simulate the cable behavior with MATLAB programming. In addition, a 1-D model is also made with the same principles. The study case network (Fig 2) with only the presence of the DC cable and a pole-to-pole short circuit at t = 0.1 s at the load location, with a duration of 100 ms, is considered to compare the models. The line current, and inner and outer HTS tapes' temperature obtained from the study case simulation during fault (short time) are depicted in Fig. 5(a), (b) and (c), respectively. In the 1-D and 2-D models a small (almost zero) heat transfer between the inner/outer HTS tapes and core/shield copper is assumed. These figures demonstrate a high similarity of results in showing the increase in line current and tapes temperature during fault for all the models, especially the 1-D and 2-D models which give almost identical outcomes. From computational effort point of view, for 40 s simulation of the cable using a workstation with Core i7 CPU and 16 GB RAM takes few seconds with lumped-parameter and 1-D model, while this takes around 5 minutes with the 2-D model. Therefore, for short times, the lumped-parameter

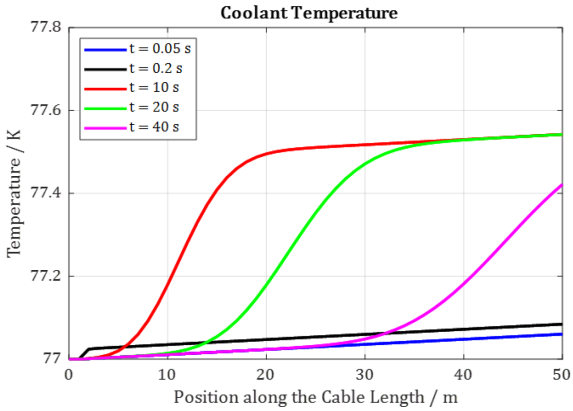

Fig. 6. LN_2 temperature profile along the cable length at different times obtained from the 2-D model.

model seems to be a fast and simple solution to simulate the cable behavior. However, in the longer simulations, the heat transfer between layers plays a significant role in the temperature variation; hence, in the case of a short-length cable, both 1-D and 2-D models give reasonable results, while in the case of a long cable, the 2-D model is the more suitable solution. For example, considering only the coolant, Fig. 6 depicts the LN_2 temperature increase along the cable length at different times. This shows the necessity of the 2-D model to monitor the cable transient behavior after a phenomena like fault.

V. Simulation of a Cable Equipped with a Fault Current Limiter

A MATLAB SIMULINK model including the lumped-parameter models of the RSFCL and cable to simulate the study case network (Fig. 2) during a fault is developed. For the cable, the model accuracy was validated with reference to the 2-D model in previous section. The results are shown in Fig. 7, which illustrates the effective assistance of the RSFCL to limit the fault current. Moreover, it is confirmed that with the presence of a fault limiter, the temperature and resistance increase in the tapes of the cable is relatively negligible, while it is significant for the tapes in the RSFCL. Therefore, the RSFCL protects the cable from any sudden temperature rise.

VI. Conclusion and Perspectives

Electric aircraft represent a promising solution for reducing CO_2 emissions in the aviation industry. Introducing a superconducting powertrain in such aircraft offers numerous advantages that could further accelerate the electrification of aviation. This study focused on superconducting fault current limiters (SFCL) and DC cables, the two components of this powertrain. The behavior of these components was simulated using MATLAB programming, and to facilitate customization and flexibility, SIMULINK models were developed. For the cable, the lumped-parameter, 1-D, and 2-D models were developed. Comparison of these models validated the accuracy of the L-P model, with reference to the 2-D model in short simulation times, while in long term, the 1-D and 2-D models are reasonable solutions. Finally, the developed SIMULINK model including both RSFCL and cable demonstrated the RSFCL effectiveness in protecting

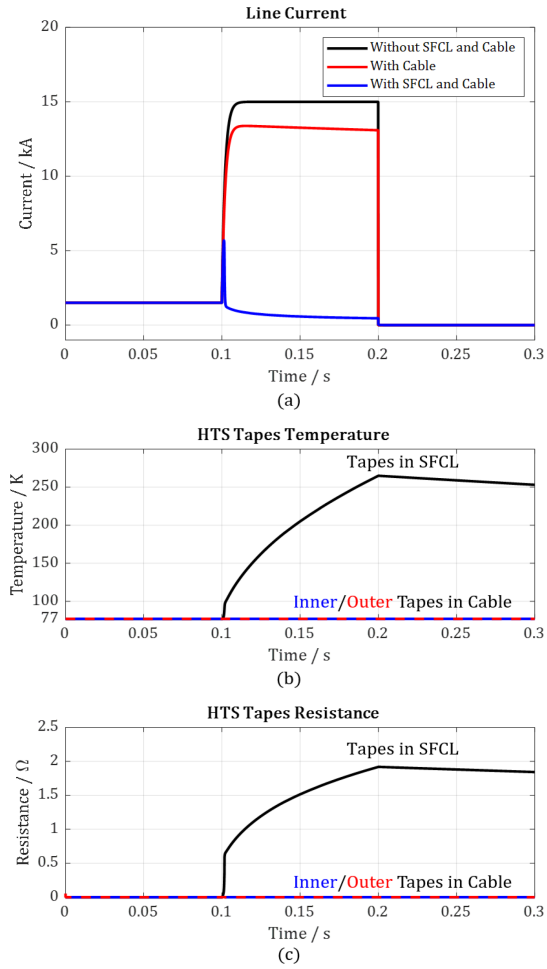

Fig. 7. Study case simulation results: (a) Line current profile demonstrating the effect of SFCL in the network with cable. (b) Tapes' temperature. (c) Tapes' resistance.

the cable and limiting the fault current. The next steps in this work will be to model other superconducting components of electric aircraft, with a particular focus on the superconducting motor.

References

[1] T. C. Cano et al., "Future of electrical aircraft energy power systems: An architecture review," *IEEE Trans. Transp. Electrific.*, vol. 7, no. 3, pp. 1915–1929, Sep. 2021, doi: 10.1109/TTE.2021.3052106.

[2] Airbus, "Global Market Forecast." Jun. 2023. Accessed: Jun. 22, 2023. [Online]. Available: https://www.airbus.com/en/products-services/commercial-aircraft/market/global-market-forecast

[3] European Commission, Directorate-General for Mobility and Transport, Directorate-General for Research and Innovation, "Flightpath 2050: Europe's vision for aviation: Maintaining global leadership and serving society's needs," *Pub. Office*, 2011, doi: 10.2777/50266.

[4] K. Kovalev, J. Nekrasova, N. Ivanov, and S. Zhurzvlev, "Design of all-superconducting electrical motor for full electric aircraft," in *Proc. Int. Conf. Electrotechnical Complexes Syst.*, 2019, pp. 1–5, doi: 10.1109/ICOECS46375.2019.8949952.

[5] C. A. Luongo et al., "Next generation more-electric aircraft: A potential application for HTS superconductors," *IEEE Trans. Appl. Supercond.*, vol. 19, no. 3, pp. 1055–1068, Jun. 2009, doi: 10.1109/TASC.2009.2019021.

[6] F. Berg, J. Palmer, P. Miller, and G. Dodds, "HTS system and component targets for a distributed aircraft propulsion system," *IEEE Trans. Appl. Supercond.*, vol. 27, no. 4, Jun. 2017, Art. no. 3600307, doi: 10.1109/TASC.2017.2652319.

[7] L. Ybanez et al., "ASCEND: The first step towards cryogenic electric propulsion," in *IOP Conf. Ser.: Mater. Sci. Eng.*, vol. 1241, 2022, Art. no. 012034, doi: 10.1088/1757-899X/1241/1/012034.

[8] J. K. Nøland, R. Mellerud, and C. Hartmann, "Next-generation cryoelectric hydrogen-powered aviation: A disruptive superconducting propulsion system cooled by onboard cryogenic fuels," *IEEE Ind. Electron. Mag.*, vol. 16, no. 4, pp. 6–15, Dec. 2022, doi: 10.1109/MIE.2022.3174332.

[9] W. T. B. de Sousa, "Transient simulations of superconducting fault current limiters," Ph.D. Dissertation, Federal University of Rio de Janeiro, Rio de Janeiro, Brazil, 2015.

[10] P. E. Sutherland, "Analytical model of superconducting to normal transition of bulk high TC superconductor BSCCO-2212," *IEEE Trans. Appl. Supercond.*, vol. 16, no. 1, pp. 43–48, Mar. 2006.

[11] F. W. Grover, *Inductance Calculations*. D. Phoenix Eds., Mineola, NY, USA: Dover Publications, 2004.

[12] W. T. B. De Sousa, E. Shabagin, D. Kottonau, and M. Noe, "An open-source 2D finite difference based transient electro-thermal simulation model for three-phase concentric superconducting power cables," *Supercond. Sci. Technol.*, vol. 34, no. 1, Dec. 2020, Art. no. 015014, doi: 10.1088/1361-6668/ABC2B0.